PHYSICAL REVIEW VOLUME 146, NUMBER 1 3 JUNE 1966

Paramagnetic Acoustic Resonance and Relaxation of Rare Earths in CaF_2†

W. I. DOBROV
Lockheed Palo Alto Research Laboratory, Palo Alto, California

(Received 29 November 1965)

Using the group-theoretical approach of Blume and Orbach, a Hamiltonian is derived for interaction between coherent acoustic waves and rare-earth ions in cubic coordination. This Hamiltonian is found in partial agreement with the phenomenological spin-phonon Hamiltonian for effective spin $S=\frac{1}{2}$ ions. Observations were made of the transmission of longitudinal and transverse 10-kMc/sec acoustic waves through rare-earth-doped CaF_2 as a function of an applied magnetic field. Magnetic-field-dependent attenuation of acoustic waves was observed for only two ions, Eu^{2+} and Dy^{3+}. In other cases only the upper limits of the acoustic absorption could be determined, and from these, lower limits of the direct-process relaxation time T_1 were estimated. These lower limits were found approximately three orders of magnitude longer than the T_1 values measured in CaF_2 at liquid-helium temperatures by the conventional pulse-saturation technique; an explanation of the discrepancy for some cases is suggested.

I. INTRODUCTION

THIS work on interaction of rare-earth ions with lattice vibrations in CaF_2 was motivated by two objectives: (1) development of an interaction Hamiltonian, which is adequately supported by theoretical arguments and which would be useful in microwave phonon work; and (2) comparison of spin-lattice relaxation-time measurements at low temperatures with the intensity of spin-lattice interaction as obtained from microwave acoustic measurements.

Calculations based on Orbach's original theory[1] of rare-earth relaxation rates were found in agreement with experimental results in several instances.[2–5] However, considering the many approximations of such calculations it is certainly desirable to know whether the measured low-temperature relaxation times are compatible with the one-phonon process. If they are strongly incompatible, clearly processes other than the direct one are effective, even if calculations based on the usual Orbach-type estimates agree in order of magnitude with the measured times.

A method of measuring the effectiveness of the one-phonon process is the paramagnetic resonant absorption of acoustic waves. This technique involves piezoelectric or magnetostrictive excitation of coherent acoustic waves at microwave frequencies and their propagation through paramagnetic crystals while sweeping the magnetic field through resonance. The magnitude of the magnetically-dependent absorption produced by the spin transitions between the Zeeman levels is a measure of the spin-lattice coupling strength, which also determines the one-phonon relaxation rate.

Until now, most experiments of this type involved magnetically diluted ions of the iron group.[6–10] The form of the phenomenological spin-phonon interaction Hamiltonian for these ions has been found in agreement with experiments[11,12] and is also well justified theoretically by the work of Van Vleck[13] and Mattuck and Strandberg.[14] In analogy with the spin Hamiltonian

$$\mathcal{H}_s=\beta\mathbf{H}\cdot\mathbf{g}\cdot\mathbf{S}+\mathbf{S}\cdot\mathbf{D}\cdot\mathbf{S} \tag{1}$$

the spin-phonon Hamiltonian is written

$$\mathcal{H}_{s-p}=\beta\mathbf{H}\cdot\mathbf{h}\cdot\mathbf{S}+\mathbf{S}\cdot\mathbf{d}\cdot\mathbf{S}, \tag{1a}$$

where tensors **h** and **d** represent the phonon modulation of the tensors **g** and **D**, respectively. Although for S-state ions in cubic fields the spin Hamiltonian does not contain spin components to the second power, i.e., it is

$$\mathcal{H}_s=\beta g\mathbf{S}\cdot\mathbf{H}+\tfrac{1}{6}a[S_x^4+S_y^4+S_z^4 -\tfrac{1}{5}S(S+1)(3S^2+3S-1)], \tag{2}$$

the spin-phonon Hamiltonian is still of the form of Eq. (1a) with the second term being dominant, as has been shown by Blume and Orbach's theoretical work[15] and by experiments.[11,12]

No rigorous theory exists which would give the general form of the interaction between a beam of acoustic waves and ions of $4f$ and $5f$ transition groups. For the rare-earth ions in cubic fields with the Γ_8 quartet lying lowest, the spin Hamiltonian is[16]

$$\mathcal{H}_s=g\beta(H_xS_x+H_yS_y+H_zS_z) +f\beta(H_xS_x^3+H_yS_y^3+H_zS_z^3), \tag{3}$$

but again it seems reasonable to take the second term

---

† Supported by the Lockheed Independent Research Fund.

[1] R. Orbach, Proc. Roy. Soc. (London) **A264**, 458 (1961); **A264**, 485 (1961).

[2] P. L. Scott and C. D. Jeffries, Phys. Rev. **127**, 32 (1962).

[3] C. Y. Huang, Phys. Rev. **139**, A241 (1965).

[4] G. H. Larson and C. D. Jeffries, Phys. Rev. **141**, 461 (1966).

[5] R. C. Mikkelson and H. J. Stapleton, Phys. Rev. **140**, A1968 (1965).

[6] E. B. Tucker, Phys. Rev. Letters **6**, 183 (1961).

[7] N. S. Shiren, Bull. Am. Phys. Soc. **7**, 29 (1962).

[8] W. I. Dobrov and M. E. Browne, Bull. Am. Phys. Soc. **6**, 508 (1961).

[9] N. S. Shiren, Phys. Rev. **128**, 2103 (1962).

[10] R. N. Claytor, P. L. Donoho, and B. Josephson, Bull. Am. Phys. Soc. **7**, 15 (1962).

[11] N. S. Shiren and E. B. Tucker, Phys. Rev. Letters **6**, 105 (1961).

[12] W. I. Dobrov, Phys. Rev. **134**, A734 (1964).

[13] J. H. Van Vleck, Phys. Rev. **57**, 426 (1940).

[14] R. D. Mattuck and M. W. P. Strandberg, Phys. Rev. **119**, 1204 (1960).

[15] M. Blume and R. Orbach, Phys. Rev. **127**, 1587 (1962).

[16] B. Bleaney, Proc. Phys. Soc. (London) **73**, 937 (1959).

of Eq. (1a) as the effective phenomenological spin-phonon Hamiltonian. The interaction term of the $\mathbf{S}\cdot\mathbf{d}\cdot\mathbf{S}$ form was also taken by Wetsel and Donoho[17] to describe the absorption of microwave ultrasonics by non-Kramers U^{4+} ions located at trigonal sites in CaF_2. They indicated that observations on the ground state of such ions can be explained in terms of a spin-phonon Hamiltonian

$$\mathcal{H}_{s-p}=\textstyle\sum_i A_iS_i\,, \quad (A_i=\text{linear functions of strains}) \tag{4}$$

but they rejected this latter form on the ground that it is not invariant under time reversal. For iron-group elements with the effective spin $S=\frac{1}{2}$ the interaction is described by the first term in Eq. (1a), as has been shown theoretically[13,14] and worked out in detail for acoustic-waves absorption in Ref. (12). It is not immediately obvious that the same form applies to $S=\frac{1}{2}$ rare-earth ions with their reversed relationship between the spin-orbit coupling and the crystalline electric field. The above examples have shown that in general there is no simple relationship between the spin Hamiltonian and the form of the spin-phonon interaction as the analogy between the Eqs. (1) and (1a) may lead one to believe. Thus it would be useful to develop a Hamiltonian which then will be either directly employed in microwave acoustic experiments, if it contains a manageable number of unknown parameters, or at least could be used to check the validity of forms of intuitively suggested phenomenological Hamiltonians.

II. INTERACTION HAMILTONIAN

Following the approach used by Blume and Orbach[15] in their work on spin-lattice relaxation of iron-group S-state ions in octahedral coordination we develop the interaction Hamiltonian for rare-earth ions in cubic coordination (fluorite structure) and plane acoustic waves. It appears that this approach can be extended without too much trouble to treat the rare earths in cubic fields of other coordinations and also to other cases of relatively high symmetry, but it certainly becomes impractical for low local symmetries.

In CaF_2 a rare-earth ion replaces the calcium and is surrounded by a cubic complex of eight fluorine ions. Acoustic waves displace the fluorines, thus producing an alternating electric field at the rare-earth site. The crystal-field interaction can be expanded in powers of a general strain ϵ:

$$\mathcal{H}_c=\mathcal{H}_{c0}+\epsilon V_c+\epsilon^2 V_c'+\cdots\,, \tag{5}$$

where

$$\mathcal{H}_{c0}=\sum_{n,m} A_n{}^m\langle r_0{}^n\rangle Y_n{}^m(\theta,\phi) \tag{5a}$$

is the static crystal field, $Y_n{}^m(\theta,\phi)$ are normalized spherical harmonics, $A_n{}^m\langle r^n\rangle$ are static crystal-field parameters, and ϵV_c, $\epsilon^2 V_c'$ are the dynamic crystal-field terms. A cubic field is characterized by only two parameters $A_4\langle r^4\rangle$ and $A_6\langle r^6\rangle$, but an acoustic wave lowers the symmetry and introduces a larger number of dynamic parameters $a_n{}^m\langle r^n\rangle$ into ϵV_c. We will neglect the terms of second and higher power in ϵ but we will be concerned with the direction of propagation and polarization of ϵ, in contrast to calculations of spin-lattice relaxation rates where ϵ is usually treated as a not-well-defined average of all thermal strains.

In the expression for orbit-lattice interaction we are interested only in terms which transform as the irreducible representations present in the vibration spectrum. Because of symmetry properties, the vibrations of an eight-fold coordinated complex transform according to irreducible representations of the O_h group as follows:

$$\Gamma_{\text{vib}}(O_h)=\Gamma_{1g}+\Gamma_{2u}+\Gamma_{3g}+\Gamma_{3u}+2\Gamma_{4u}+2\Gamma_{5g}+\Gamma_{5u}\,. \tag{6}$$

The irreducible representations of odd parity can be omitted, since corresponding matrix elements which involve wave functions of equal parity, are zero. If $J>4$, rare earths in a cubic environment may relax through the totally symmetric Γ_{1g} vibration which could mix different electronic states of the same cubic representation. In this treatment we are concerned with the ground-state transitions, which are usually affected by the mixing with the first excited state to a considerably greater extent than by admixtures of the higher lying states. A rather special situation where the ground state and the first excited state belong to the same irreducible representation occurs in cubic fields only in a few cases[18] and thus we can omit the Γ_{1g} vibration without an appreciable loss of generality.

As shown in the Appendix, one of the Γ_{5g} vibrations, $B\Gamma_{5g}$, is irrelevant to our problem; therefore we need to consider only Γ_{3g} and $A\Gamma_{5g}$ representations. Forming combinations of strain components and combinations of spherical harmonics transforming according to these representations, we write the general interaction Hamiltonian

$$\mathcal{H}_{s-p}=\sum_{\substack{i=2,4,6;\\ j=1,2}} a_{1i}b_{1ij}q_j+\sum_{\substack{i=2,4,6;\\ l=3,4,5}} a_{2i}b_{2il}q_l +a_{36}\sum_{l=3,4,5} b_{36l}q_l\,. \tag{7}$$

Here b_{ijk} and q_i are appropriate combinations of spherical harmonics and strains, respectively, and are given in the Appendix. The dynamic crystal-field coefficients a_{mn} are associated each with a particular irreducible representation and an orbital quantum number n, where $n=2$, 4, 6. With known wave functions, the matrix elements of Eq. (7) can be evaluated, and if the strain-spin interaction is experimentally measured, the coefficients a_{mn} are determined.

---

[17] G. C. Wetsel and P. L. Donoho, Phys. Rev. **139**, A334 (1965).

[18] K. R. Lea, M. J. M. Leask, and W. P. Wolf, J. Phys. Chem. Solids **23**, 1381 (1962).

III. RELATION BETWEEN ACOUSTIC ABSORPTION COEFFICIENT AND RELAXATION

Accurate knowledge of wave functions is not necessary for comparison of directly measured relaxation times to those obtained from acoustic experiments, if paramagnetic absorption coefficients for a number of longitudinal and transverse modes are known. This is especially true for two-level systems where a simple relationship exists between resonant acoustic absorption and thermal relaxation via the direct process. Pertinent quantities for these phenomena are the products of acoustic and thermal strains multiplied by spin-lattice coupling parameters and by matrix elements of angular-momentum operators, operating on the same wave functions in both cases. Such products essentially are corresponding transition probabilities and for the acoustic transition probability we write

$$W_{ac}=[g_s(\nu)/4\hbar^2]|\langle\psi(m)|L_{ac}\epsilon_{ac}|\psi(m')\rangle|^2\ \mathrm{sec}^{-1}, \tag{8}$$

where $g_s(\nu)$ is the shape function of the acoustic interaction; $\psi(m)$, $\psi(m')$ are the wave functions of the two levels involved, and $L_{ac}\epsilon$ is the Hamiltonian, Eq. (7), for a specific acoustic mode. Here ϵ_{ac} is the peak value of the strain component associated with this mode and L_{ac} is the operator describing the interaction between the acoustic wave and the ions. Since matrix elements of the type shown in Eq. (8), with $L_T\epsilon_T$ replacing $L_{ac}\epsilon_{ac}$, describe the thermally induced transition, we have, taking the average over all acoustic modes: $\bar{L}_{ac}=L_T$. Therefore, the two transition probabilities are simply related by the squares of strain amplitudes

$$W_T=\bar{W}_{ac,\,\mathrm{long}}\left(\frac{\epsilon_T}{\epsilon_{ac}}\right)^2_{\mathrm{long}}+\bar{W}_{ac,\,\mathrm{tr}}\left(\frac{\epsilon_T}{\epsilon_{ac}}\right)^2_{\mathrm{tr}}. \tag{9}$$

We replace $\epsilon_T^2/\epsilon_{ac}^2$ by the ratio of respective energy densities and express the energy density of thermal phonons through the mode and occupation numbers. Then with $W_T=\frac{1}{2}T_1$, where T_1= direct relaxation time and using the definition of the acoustic absorption coefficient

$$\begin{aligned}\alpha&\equiv\Delta P/P=\Delta n h\nu W_{ac}/P,\\ P&=\tfrac{1}{2}\rho v_{l,t}^3\epsilon_{ac}^2,\end{aligned} \tag{10}$$

where α is the absorption coefficient, ΔP is the absorbed acoustic power, P is the acoustic intensity, Δn is the ion-population difference between the two magnetic sublevels, and $v_{l,t}$= sound velocity of longitudinal and transverse waves, respectively, we finally obtain

$$\frac{1}{T_1}=\frac{8\pi\nu kT}{g_s(\nu)\Delta nh}\left[\frac{\bar{\alpha}_l}{\bar{v}_l^2}+\frac{2\bar{\alpha}_t}{\bar{v}_t^2}\right]. \tag{11}$$

When measurements of relaxation time by saturation are compared to acoustic results in multilevel systems, the situation becomes more complex, since there are, in general, several relaxation rates in the return to equilibrium. Rate equations and, in principle, Eq. (11) still can be used with α's now being absorption coefficients between various levels; but a better and a more thorough approach would be to obtain the wave functions, to measure the spin-lattice coupling parameters and to use them both in calculation of T_1 by taking into account a large number of acoustic modes. Shiren[19] found a satisfactory agreement between measured T_1 and his ultrasonic data by considering three different relaxation rates for iron-group ions in MgO. However, even the simplified approach outlined above and the measurement of coupling parameters for one or two acoustic modes[6,20] yielded results which agree fairly well with T_1 values measured in dilute ruby and with more detailed calculation based on uniaxial-stress data.[21] Most rare-earth ions in $\mathrm{CaF_2}$ are effectively two-level systems; thus Eq. (11) together with the measurements of acoustic absorption coefficient for one longitudinal and one transverse mode along crystalline symmetry axes should provide an adequate indication as to the order of magnitude of the relaxation rates due to the one-phonon process.

IV. EXPERIMENTAL MEASUREMENTS

Calcium fluoride was chosen for these experiments because its mechanical properties make it suitable for acoustic work and also because the relaxation times and spin resonance of rare earths in it have been studied extensively.[22–24] The charge compensation and, as a result of it, the presence of sites of different local symmetries could be a drawback of $\mathrm{CaF_2}$ as a host material; on the other hand the hardness and the large size of crystals, which readily lend themselves to optical polishing and bonding, are important advantages. Trivalent rare-earth ions can be incorporated in other host crystals without charge compensation, but usually small size, softness, hygroscopic properties, or low local symmetry added to an abundance of magnetically nonequivalent sites make acoustic experiments in such crystals very difficult.

The apparatus employed in these experiments has been described in detail elsewhere.[12] The method is similar to the one used by Shiren and Tucker,[6,7,9] who made the first measurements of the interaction of ultrasonics with spins after the development of microwave

---

[19] N. S. Shiren, in *Magnetic and Electric Resonance and Relaxation*, edited by J. Smidt (Interscience Publishers, Inc., New York, 1963).

[20] W. I. Dobrov and M. E. Browne, in *Proceedings of the First International Conference on Paramagnetic Resonance, Jerusalem, 1962*, edited by W. Low (Academic Press Inc., New York, 1963).

[21] P. L. Donoho, Phys. Rev. **133**, A1080 (1964).

[22] B. Bleaney, P. M. Llewellyn, and D. A. Jones, Proc. Phys. Soc. (London) **B69**, 858 (1956).

[23] J. M. Bauer, W. Hayes, and M. C. M. O'Brien, Proc. Roy. Soc. (London) **A254**, 273 (1960).

[24] M. J. Weber and R. W. Bierig, Phys. Rev. **134**, A1492 (1964); R. W. Bierig, M. J. Weber, and S. I. Warshaw, *ibid.* **134**, A1504 (1964).

TABLE I. Comparison of T_1 obtained from acoustic experiments to the values measured by pulse-saturation technique, $T=1.6°K$; $f=9.6$ kMc/sec; $\mathbf{k}\|[100]$.

Ion	Mode	Concentration (%)	$\alpha_{\max}$ (cm^{-1})	Acoustic T_1 tetrag. (sec)	Acoustic T_1 cubic (sec)	Pulse saturation T_1 tetrag. (sec)	Pulse saturation T_1 cubic (sec)
Ce^{3+}	longitudinal	0.1	≤ 0.02	28		2×10^{-3}[a]	
Pr^{3+}	longitudinal	0.5	≤ 0.03				
Pr^{3+}	transverse	0.5	≤ 0.06				
Nd^{3+}	longitudinal	0.1	≤ 0.01	8		0.5×10^{-3}[a]	
Nd^{3+}	transverse	0.5	≤ 0.04				
Eu^{2+}	longitudinal	0.3	$=0.1$		7		90×10^{-3}[b]
Dy^{3+}	longitudinal	0.16	$=10.5$ *db*		$\leq 10^{-3}$		$\leq 3\times10^{-6}$[a]
Ho^{3+}	longitudinal	0.2	≤ 0.02				
Er^{3+}	longitudinal	0.15	≤ 0.02	5	7	2×10^{-3}[a]	$0.6\cdot10^{-3}$[a]
Er^{3+}	transverse	0.15	≤ 0.04				
Yb^{3+}	longitudinal	0.2	≤ 0.05	6	19	1×10^{-3}[a]	$0.4\cdot10^{-3}$[a]

[a] Reference 24. [b] Reference 3.

acoustic techniques by Jacobsen[25] and by Bömmel and Dransfeld.[26]

We studied the interaction with longitudinal waves by bonding samples of doped CaF_2 (purchased from Optovac, Inc.) to quartz rods or plates in which 10-kMc/sec acoustic waves were generated. The paramagnetic spectrum of a given specimen was previously recorded and the magnetic field was varied over the range of the spectrum while observing the amplitude of the transmitted acoustic pulses. When relationship between acoustic frequency and magnetic field satisfies the magnetic-resonance condition, a decrease of acoustic intensity is observed provided the interaction is sufficiently strong. If the magnetic-resonance region was covered and no magnetically-dependent absorption has been observed, the upper limit of the ion-acoustic-wave interaction can be established from the experimental sensitivity.

Most experiments with longitudinal waves were conducted with a 45-deg angle between the applied magnetic field and propagation direction, but searches at other angles, θ between 0 and 90 deg, were also made. Only in two instances, for divalent europium[12] and trivalent dysprosium,[27] was positive identification of longitudinal-wave absorption made; in other cases we were able to determine only the upper limits of the absorption coefficients. The maximum possible values of the absorption are given in Table I; the limits vary from ion to ion because of variations in bonding, ultrasonic generation, and detection efficiency.

Dysprosium with its strong interaction presents a sharp contrast to other ions. We attribute the difference to the fact that Dy^{3+} is actually found on cubic sites in CaF_2 where its ground state is a Γ_8 quartet, whereas other Kramers ions in Table I, with exception of Eu^{2+}, have doublets lying lowest. For Dy^{3+} transitions can, therefore, occur at 10 kMc/sec between the levels which are not Kramers conjugates, thus explaining the relatively large transition probabilities. This factor, together with zero field splitting and line broadening caused by the slight departures from local cubic symmetry, explains the qualitative features of the acoustic spectrum shown in Fig. 1.

Experimental sensitivity, which was considerably enhanced by selective integration of transmitted pulses, allowed us to set such limiting values of acoustic ab-

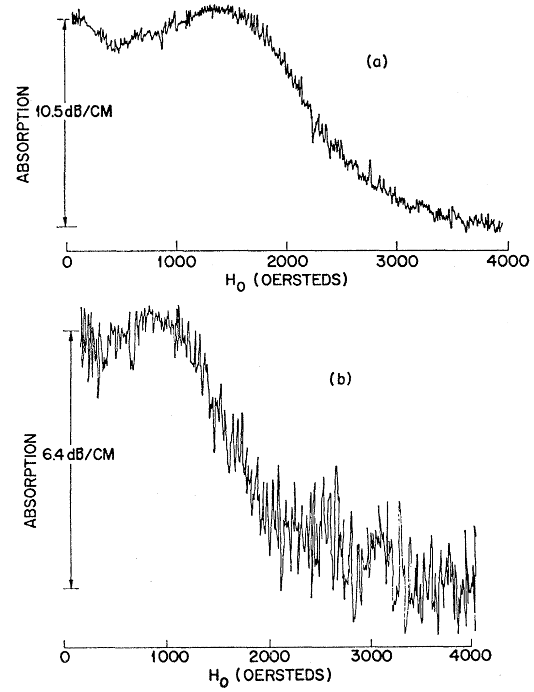

FIG. 1. Paramagnetic absorption of longitudinal acoustic waves in 0.16% Dy-doped CaF_2. $T=1.6°K$; $f=9.6$ kMc/sec; $\theta=60°$; $\mathbf{k}\|[100]$. (a) Before annealing, (b) after annealing.

---

[25] E. H. Jacobsen, Phys. Rev. Letters **2**, 249 (1959).

[26] H. E. Bömmel and K. Dransfeld, Phys. Rev. Letters **1**, 234 (1958).

[27] W. I. Dobrov, Phys. Rev. Letters **15**, 789 (1965).

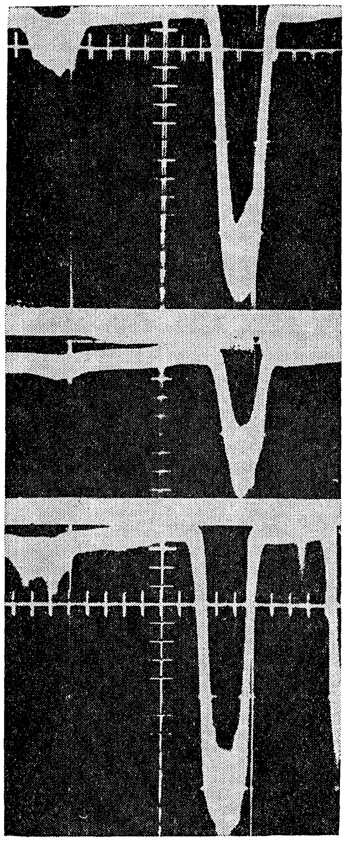

FIG. 2. Demonstration of paramagnetic resonant absorption of 10-kMc/sec transverse acoustic waves generated by ferromagnetic resonance in a thin film. Cobalt film was deposited on 0.17% concentrated ruby substrate. Upper picture: above ruby resonance $H=5280$ Oe; middle picture: on resonance $H=5200$ Oe; lower picture: below resonance $H=5120$ Oe.

sorption on the basis of longitudinal measurements, that much longer relaxation times than those reported in Ref. 24 seem to follow, provided that interaction with transverse modes is not significantly stronger. A stronger transverse wave absorption coupled with the lower value of sound velocity than that of longitudinal waves, could easily make the dominant contribution to relaxation rate in Eq. (11). Transverse wave experiments are somewhat complicated by the difficulty of bonding and coupling 10-kMc/sec ($\lambda_s=3500$ Å) transverse waves in and out of nonpiezoelectric samples. The problem of bonding can be avoided if thin magnetic films are deposited on polished samples and are used as transducers for generation and detection of acoustic pulses. But then a new problem arises since a magnetic field is needed for the two sometimes incompatible purposes, i.e., for wave generation and also for the study of wave interaction. However, no conflict exists if thin, $l=1800$ Å cobalt films are used in which transverse waves can be produced by ferromagnetic resonance over a field region of several thousands of oersteds. The paramagnetic absorption is then easily observed as a relatively narrow dip on a broad background, as Fig. 2 demonstrates for ruby at approximately the same Cr^{3+} concentration as rare-earth concentrations in our CaF_2 samples. In these experiments one film was used for both detection and generation of signals. It was placed in a strong circularly polarized microwave magnetic field and the sample was rotated about the film normal. The latter operation substantially improved the signal intensity, evidently by allowing us to select an orientation of maximum spatial coherence of acoustic waves. Application of this technique and work with the transverse waves proved to be more difficult than with the longitudinal ones, mainly because the efficiency of phonon generation by cobalt films over the desired broad-field range is strongly dependent on surface finish of the substrate and on deposition techniques. Still, the magnetostrictive-film techniques as compared to the piezoelectric ones (including the piezoelectric films) have the advantage of providing means to excite different acoustic modes by merely changing the angle between the film normal and the magnetic field, thereby allowing one to switch from circularly to linearly polarized transverse, or even to longitudinal waves.[28]

No positive observation of magnetically-dependent absorption of transverse waves was made, thus leading only to the determination of upper values of the effect as shown in Table I. The magnitudes of T_1 of Nd^{3+} and Er^{3+} reported in Ref. 24 are such, that had they been due to one-phonon relaxation, proceeding primarily through transverse modes, the resonant absorption of these modes would have been approximately three orders of magnitude larger than our sensitivity limit.

We may consider the possibility that direct relaxation proceeds through some modes which are more efficient than the ones we have generated. However, since such modes would have to be orders of magnitude stronger coupled to the spins, we must discard this possibility and conclude that at 1.6°K Nd^{3+} and Er^{3+} do not relax primarily through a one-phonon process. Although transverse-wave data are lacking, it seems reasonable to draw the same conclusion with regard to Ce^{3+} and Yb^{3+} ions, for which T_1 values in Table I were obtained by assuming $\alpha_l \approx \alpha_t$ in Eq. (11).

Experiments on non-Kramers Ho^{3+} ion were conducted primarily in order to ascertain that the strong interaction of dysprosium, Fig. 1, is not due to Dy^{2+} ion, with which Ho^{3+} is isoelectronic, and which may be present in small quantity in dysprosium-doped samples. Absorption of longitudinal and transverse ultrasonics by the other non-Kramers ion Pr^{3+} was searched for at $g=2$, where an EPR line was observed; only longitudinal waves could be used in investigations near $H=0$, where zero-field electromagnetic transitions were reported.[29] Lower limits of T_1 could not be obtained from the upper limits of α in this case, since the ion distribution between the sites and the width of the zero-field line are not known. The acoustic measurement on the S state, $S=\frac{7}{2}$ Eu^{2+} ion has been reported elsewhere[12] and for completeness is included in Table I,

---

[28] M. H. Seavey, Jr., IEEE Trans. Ultrasonics Eng. 10, 49 (1963).

[29] D. E. Kaplan (private communication).

from which it is evident that in this case also the direct-relaxation process is not the dominant one.

V. DISCUSSION

The results of experimental measurements are not sufficient to test the validity of the interaction Hamiltonian, Eq. (7). Paramagnetic acoustic absorption was actually observed for only two ions Eu^{2+} and Dy^{3+} and they present rather special cases. There is not much doubt about the validity of the Hamiltonian of this form for S-state ions, as shown by Blume and Orbach's work[15] and by experiments, but Dy^{3+} experimental data cannot be used to test the theory.

For such a comparison the field symmetry at the sites occupied by the absorption centers has to be known. As angle θ was varied, the Dy^{3+} absorption was observed to reach a maximum at $\theta=45°$, as is expected for longitudinal $\Delta m=1$ transitions, but the interaction pattern was not symmetric with respect to that angle. An angular behavior of this type would result if unresolved $\Delta m=1$ and $\Delta m=2$ transitions with their different angular dependencies are observed simultaneously. Although this complicates the determination of the symmetry type from the angular variations, we know that the local symmetry must be essentially cubic. In the tetragonal field of CaF$_2$ the quartet separates in two doublets, the separation being of such magnitude that x-band resonances can occur only in fields $H=2300$ Oe or higher.[30] The confirmation is also found in the observations shown in Figs. 1(a) and 1(b): The lower figure shows an absorption decrease upon sample annealing, which converts some cubic sites into axial ones.[31] On the other hand, in a purely cubic environment the ground Γ_8 state is degenerate and, in contradiction to Fig. 1, α should be zero for $H=0$. Evidently the observed pattern can be explained only by local departures from cubic symmetry, which, although small, are the cause of the important features of the spectrum. But Eq. (7) applies to cubic environment, and furthermore, in order to compare it to the experiment, resolution and identification of observed transitions are necessary. The spectrum is unresolved because acoustic lines are much broader than the Dy^{3+} electromagnetic absorption lines,[30] $\Delta H\approx 40$ Oe. Presumably the main differences between the two spectra, such as zero-field acoustic absorption, are caused by relatively few ions with extremely strong coupling to the lattice.

Even though at present we cannot verify experimentally the general applicability of Eq. (7) to rare-earth ions in a cubic environment, that equation, in view of its more rigorous derivation than phenomenological expressions, can be used to test their validity. Many rare-earth ions have effective spin $S=\frac{1}{2}$ and for them the phenomenological Hamiltonian will be only the first term of Eq. (1a). This Hamiltonian, operating now on effective spin wave functions, rather than on real wave functions, as the operator Eq. (7) does, will contain a smaller number of independent parameters and will be simpler to use. The tensor $\mathbf{h}$, when expanded in acoustic strains, in cubic case will contain only three coupling parameters, in terms of which relaxation times can be calculated, provided the use of a Hamiltonian of this form can be justified. If the form is correct, we expect the field and the angular dependence of acoustic absorption coefficients, i.e., of transition probabilities, to be the same for the $\beta\mathbf{H}\cdot\mathbf{h}\cdot\mathbf{S}$ form as for Eq. (7).

To estimate the latter, consider the eigenfunctions of the static crystalline field $|a_0\rangle$, $|b_0\rangle$ belonging to the lowest doublet, and $|c_0\rangle$, $|d_0\rangle$ belonging to the next-lying state.

The Zeeman perturbation is

$$\mathcal{H}_z=\beta\Lambda\mathbf{H}\cdot\mathbf{J}\,, \tag{12}$$

where Λ is the Landé factor. This perturbation mixes the wave functions which, if the g-factor is isotropic, in the limit of infinite separation between the two groups of levels are given

$$\begin{aligned}
|\psi_a{}^0\rangle&=\frac{1}{\sqrt{2}}[(1+\cos\theta)^{1/2}|a_0\rangle-(1-\cos\theta)^{1/2}|b_0\rangle],\\
|\psi_c{}^0\rangle&=\frac{1}{\sqrt{2}}[(1-\cos\theta)^{1/2}|a_0\rangle+(1+\cos\theta)^{1/2}|b_0\rangle],\\
|\psi_c{}^0\rangle&=\frac{1}{\sqrt{2}}[(1+\cos\theta)^{1/2}|c_0\rangle-(1-\cos\theta)^{1/2}|d_0\rangle],\\
|\psi_d{}^0\rangle&=\frac{1}{\sqrt{2}}[(1-\cos\theta)^{1/2}|c_0\rangle+(1+\cos\theta)^{1/2}|d_0\rangle].
\end{aligned} \tag{13}$$

θ is the angle between magnetic field and $x\|[100]$ axis, along which longitudinal waves are propagated. For finite separation Δ, the Zeeman term mixes $|\psi_c{}^0\rangle$ and $|\psi_d{}^0\rangle$ with $|\psi_a{}^0\rangle$ and $|\psi_b{}^0\rangle$. The eigenfunctions are then

$$\begin{aligned}
|\psi_a\rangle=|\psi_a{}^0\rangle-(\beta\Lambda/\Delta)\langle\psi_a{}^0|\mathbf{H}\cdot\mathbf{J}|\psi_c{}^0\rangle|\psi_c{}^0\rangle&\\
-(\beta\Lambda/\Delta)\langle\psi_a{}^0|\mathbf{H}\cdot\mathbf{J}|\psi_d{}^0\rangle|\psi_d{}^0\rangle&,\\
|\psi_b\rangle=|\psi_b{}^0\rangle-(\beta\Lambda/\Delta)\langle\psi_b{}^0|\mathbf{H}\cdot\mathbf{J}|\psi_c{}^0\rangle|\psi_c{}^0\rangle&\\
-(\beta\Lambda/\Delta)\langle\psi_b{}^0|\mathbf{H}\cdot\mathbf{J}|\psi_d{}^0\rangle|\psi_d{}^0\rangle&.
\end{aligned} \tag{14}$$

With magnetic field components

$$\begin{aligned}
H_x&=H_0\sin\theta\,,\\
H_y&=0\,,\\
H_z&=H_0\cos\theta\,,
\end{aligned} \tag{15}$$

---

[30] R. W. Bierig and M. J. Weber, Phys. Rev. **132**, 164 (1963).

[31] E. Friedman and W. Low, J. Chem. Phys. **33**, 1275 (1960).

we compute the field and the angular dependence of the transition probability for ϵ_{xx} longitudinal waves using Eq. (7):

$$W_{ac}=[g_s(\nu)/4\hbar^2](2\beta\Lambda H_0/\Delta)^2[|\langle b_0|J_x|c_0\rangle| \\ +|\langle a_0|J_z|c_0\rangle|]^2|\langle a_0|\mathcal{H}_{s-p}|c_0\rangle|^2\sin^2\theta\cos^2\theta. \quad (16)$$

This is the same field and angular dependence that was obtained in Eq. (18), Ref. 12 for a longitudinal ϵ_{xx} wave in a medium with an isotropic g factor, when the effective interaction term is $\beta\mathbf{H}\cdot\mathbf{h}\cdot\mathbf{S}$. The agreement is also found for other longitudinal waves, but for transverse waves angular dependences computed by the two procedures are different. For the transverse wave $\epsilon_{yz}\neq0$, and all others $\epsilon_{ij}=0$, we obtain from Eq. (7) the transition probability which is proportional to

$$|[\langle a_0|J_z|c_0\rangle\cos^2\theta-\langle b_0|J_x|c_0\rangle\sin^2\theta]|^2,$$

whereas the phenomenological Hamiltonian yields the transition probability proportional only to $\cos^2\theta$. Thus we conclude, that until more work is done to prove the applicability of Eq. (1a) to the rare-earth ions, it should be treated with some caution.

In theoretical calculations of the spin-lattice relaxation times, even when wave functions are well known, correct estimation of dynamic crystal-field parameters remains a serious problem. Good progress was made since Orbach suggested approximating the dynamic parameters by the static ones, an approach which was somewhat modified by the inclusion of normalizing factors.[2] Some researchers[3,4] use still another scheme, where static parameters are multiplied by the factor $n+1$, which appears if a point-charge model is assumed. Calculations of relaxation rates for different processes were compared to experiments and sometimes it was found that a certain scheme may yield a good agreement for the direct process, while the agreement for Orbach process may be very poor, and the converse situation arises if another scheme is used. Depending on the choice of the method for obtaining dynamic crystal-field parameters, variations in relaxation times of two orders of magnitude could be introduced.[3] Additional calculational uncertainties arise from lack of knowledge regarding the phase coherence of various dynamic terms, from the necessity (sometimes) of taking into account the contributions of excited J multiplets, and from incomplete information concerning wave functions. This lack of knowledge has even produced different identifications of energy states, which were then used for relaxation-time calculations CaF_2.[32] Clearly, the most direct and unambiguous verification of our understanding of relaxation processes would be through comparison of relaxation times with accurately and directly measured spin-lattice coupling coefficients, such as those which can be obtained in acoustic or uniaxial-stress experiments. That in some instances our understanding is not complete, is clear from the Table I. Bierig, Weber, and Warshaw measured a low-temperature T_1 which clearly is too short to be a one-phonon process, even if it exhibits a T^{-1} dependence.

The question arises: What processes are effective and why is the low-temperature T_1 in CaF_2 so short? It is likely that no single explanation exists and for different ions, or group of ions, different mechanisms are effective. Thus, although low-temperature T_1 data for Er^{3+} deviate from exponential behavior, they do not establish the T^{-1} dependence either,[24] indicating that at the lowest measured temperature the Orbach process may still be operative. A factor significantly shortening the relaxation time of Ce^{3+}, Nd^{3+}, and Sm^{3+} ions could be the strong coupling to the lattice which is characteristic for the Γ_8 states as observed for Dy^{3+} (Fig. 1). In the liquid-helium range Bierig and Weber[30] obtained for Dy^{3+} a T_1 of microseconds which at 4°K they attributed to the Orbach process involving the closely lying Γ_7 state. Since this process decreases exponentially with temperature, they believe that at $T\simeq2$°K the dominant mechanism may be the two-step transitions involving states within the Γ_8 quartet, i.e., the same states between which we observed the acoustic absorption. Beyond saying that on the basis of acoustic data the direct T_1 should be milliseconds or less, we cannot estimate its value and compare it to the Bierig and Weber magnetic-resonance measurement, because of lack of correspondence between the acoustic and the electromagnetic spectra. It is certain, however, that in CaF_2 the relaxation of rare-earth ions in a Γ_8 ground state is orders of magnitude faster than of ions occupying an isolated Kramers doublet. The ground states of Ce^{3+}, Nd^{3+}, and Sm^{3+} in tetragonal crystalline fields are doublets but in the cubic field of CaF_2 they are quartets. No effect similar to that of Dy^{3+} could be observed for these ions, however, since it is virtually impossible to place them, especially Nd^{3+} and Ce^{3+}, in sites of cubic symmetry due to their sizes. Nevertheless, some portion of ions will occupy cubic sites, and, although too small in number to produce measurable EPR or acoustic-resonance signals, may serve as an important relaxation channel for the slowly relaxing ions on axial sites. If the cross relaxation between the two species is fast enough, the resultant relaxation time may exhibit T^{-1} and concentration dependence, as has been observed.[24] On the other hand, if the cross-relaxation rate is significantly slower than the relaxation rate of the fast species, this explanation fails and no T^{-1} dependence is expected in general. In connection with this the Bierig, Weber, and Warshaw T_1 measurements as a function of Ce^{3+} concentration are of interest: For Ce^{3+} concentration range 0.08% to 1.6%, the product T_1T varied from 3.2×10^{-3} to 4×10^{-5} sec. These results are significant in two respects:

---

[32] G. A. Bogashev, Izv. Vysshikh Uchebn. Zavedenii 3, 95 (1965).

Firstly, they exhibit strong effects of cross relaxation, which is crucial for the above-given argument; secondly, although the cross relaxation to the exchange coupled pairs may play a role, especially at the higher concentrations, it is perhaps the cross relaxation to Γ_8 ions on cubic sites that is of importance at lower and intermediate concentrations. This argument is further supported by the fact that for several different Yb samples, no effects were observed which indicated the presence of any cross relaxation.[24] Evidently the effects of exchange coupled pairs were negligible and there could be no Γ_8 ions to cross-relax to, since the ground state of Yb^{3+} in a cubic field is a doublet. Of course, such explanation raises the question, how to account for the relaxation-time discrepancy of Yb, Table I. We cannot answer this question, except by noting that Yb is somewhat unique among the other rare-earth ions in CaF_2, in that its cubic resonances are observable at temperatures as high as 115°K, and that even outside the liquid-helium range, for $T=10$ to 20°K, its relaxation time is several orders of magnitude shorter than expected. Thus, although for an unambiguous solution of this problem quantitative data on cross relaxation and on direct relaxation of Γ_8 states are needed, it seems likely that the combination of the two processes may offer a partial explanation of the discrepancy between the acoustic and the pulse-saturation measurements. If the proposed mechanism is operative then in some instances the presence of Γ_8 ions as an impurity may noticeably affect the relaxation. Finally, the T_1 difference in Table I for the Eu^{2+}, $S_{7/2}$ ion may be due to the relaxation proceeding via multiphonon transitions between the eight spin levels of the ground state.

Recently techniques have been developed for doping CaF_2 with divalent rare earths, which are thus subjected to purely cubic environment. The advent of CdS transducers for transverse and longitudinal waves will enhance the sensitivity and the flexibility of microwave acoustic work. Experiments combining these two developments should present an opportunity for experimental verification of Eq. (7) and for measurement of various coupling parameters, from which reasonably accurate direct-process relaxation rates could be obtained.

ACKNOWLEDGMENTS

The author wishes to express his appreciation to Professor C. D. Jeffries and to Dr. G. F. Herrmann for stimulating and useful discussions, and to G. Huling for skillful preparation of samples.

APPENDIX

Consider normal coordinates transforming as rows of Γ_{3g}, $A\Gamma_{5g}$, and $B\Gamma_{5g}$ irreducible representations. The dimensionality of Γ_{3g} and of Γ_{5g} is, respectively, 2 and 3; there are thus eight normal coordinates which can be found by means of projection operators[33] in terms of ordinary ion coordinates

$$x_1, y_1, z_1;\quad x_2, y_2, z_2;\quad \cdots, x_8, y_8, z_8.$$

With the rare-earth ion at the origin, we express now the ligand ions coordinates through displacements u_i, v_i, w_i, and equilibrium coordinates x, y, z as follows:

$$\begin{array}{lll} x_1=x+u_1, & x_2=-x+u_2, & x_3=-x+u_3\cdots, \\ y_1=y+v_1, & y_2=y+v_2, & y_3=-y+v_3\cdots\text{etc.}, \\ z_1=z+w_1, & z_2=z+w_2, & z_3=z+w_3. \end{array} \tag{A1}$$

For a uniform deformation, displacements are related to the strains by

$$\begin{aligned} u&=\epsilon_{xx}x+\tfrac{1}{2}\epsilon_{xy}y+\tfrac{1}{2}\epsilon_{zx}z, \\ v&=\tfrac{1}{2}\epsilon_{xy}x+\epsilon_{yy}y+\tfrac{1}{2}\epsilon_{yz}z, \\ w&=\tfrac{1}{2}\epsilon_{zx}x+\tfrac{1}{2}\epsilon_{zy}y+\epsilon_{zz}z. \end{aligned} \tag{A2}$$

When relations (A1) and (A2) are substituted in the expressions for normal modes transforming as $B\Gamma_{5g}$, they vanish identically. This means that normal modes $B\Gamma_{5g}$ correspond to nonuniform deformation, which must be described by spatial distribution of time-varying strains. Since we are interested in interaction with plane-wave modes, characterized by a uniform strain, the $q(B\Gamma_{5g})$ vibrations are not part of our Hamiltonian. Thus the only effective modes we have to be concerned with are $q(\Gamma_{3g})$ and $q(A\Gamma_{5g})$. The problem now becomes similar to that of an octahedral complex where vibrations of only one Γ_{5g} type occur.[15] The normal modes expressed in terms of linear combinations of strains, referred to crystallographic axes, are

$$\begin{aligned} q_1(\Gamma_{3g})&=\tfrac{1}{2}(2\epsilon_{zz}-\epsilon_{xx}-\epsilon_{yy}), \\ q_2(\Gamma_{3g})&=\tfrac{1}{2}\sqrt{3}(\epsilon_{xx}-\epsilon_{yy}), \\ q_3(A\Gamma_{5g})&=-i(\sqrt{\tfrac{3}{2}})(\epsilon_{yz}+i\epsilon_{xz}), \\ q_4(A\Gamma_{5g})&=i\sqrt{3}\epsilon_{xy}, \\ q_5(A\Gamma_{5g})&=i(\sqrt{\tfrac{3}{2}})(\epsilon_{yz}-i\epsilon_{xz}). \end{aligned} \tag{A3}$$

For these combinations of strains with appropriate transformation properties, we select out of the general expansion of crystalline potential only such linear combinations of spherical harmonics that transform according to Γ_{3g} and Γ_{5g}. The interaction Hamiltonian is then the sum of combinations of spherical harmonics, each of which is multiplied by a potential coefficient (to be determined by experiment) and by q belonging to the same irreducible representation.

In view of the usual symmetry considerations and the f-electron wave functions, spherical harmonics of order $n=2$, 4, and 6 need be considered. The following linear combinations of spherical harmonics can be used as basis functions for irreducible representations of

---

[33] C. Y. Huang and M. Inoue, J. Phys. Chem. Solids **25**, 889 (1964).

interest[34]:

For Γ_{3g}, $n=2$

$$b_{121}=(2\sqrt{\pi}/\sqrt{5})Y_2^0(\theta,\phi),$$
$$b_{122}=(2\sqrt{\pi}/(10)^{1/2})(Y_2^2+Y_2^{-2}). \qquad \text{(A4)}$$

Here the first index denotes the irreducible representation ($\Gamma_{3g}=1$, $\Gamma_{5g}=2$, $\Gamma_{5g}'=3$; Γ_{5g}' occurs only for $n=6$, see below) the second index is n; and the third one corresponds to q_i, Eq. (A3).

$n=4$:

$$b_{141}=\frac{2\sqrt{\pi}}{3}\left(-\frac{\sqrt{5}}{2\sqrt{3}}Y_4^0+\frac{\sqrt{7}}{2\sqrt{6}}Y_4^4+\frac{\sqrt{7}}{2\sqrt{6}}Y_4^{-4}\right),$$

$$b_{142}=\frac{2\sqrt{\pi}}{3}\left(\frac{Y_4^2+Y_4^{-2}}{\sqrt{2}}\right);$$

$n=6$:

$$b_{161}=\frac{2\sqrt{\pi}}{(13)^{1/2}}\left\{\frac{\sqrt{7}}{2\sqrt{2}}Y_6^0+\tfrac{1}{4}(Y_6^4+Y_6^{-4})\right\},$$

$$b_{162}=\frac{2\sqrt{\pi}}{(13)^{1/2}}\left\{\frac{\sqrt{5}}{4\sqrt{2}}(Y_6^2+Y_6^{-2})+\frac{(11)^{1/2}}{4\sqrt{2}}(Y_6^6+Y_6^{-6})\right\}.$$

For Γ_{5g}, $n=2$:

$$b_{223}=\frac{2\sqrt{\pi}}{\sqrt{5}}Y_2^{-1},$$

$$b_{224}=\frac{2\sqrt{\pi}}{(10)^{1/2}}(Y_2^2-Y_2^{-2}),$$

$$b_{225}=-\frac{2\sqrt{\pi}}{\sqrt{5}}Y_2^1;$$

$n=4$:

$$b_{243}=\tfrac{1}{6}(2\pi)^{1/2}(7^{1/2}Y_4^3-Y_4^{-1}),$$
$$b_{244}=\tfrac{1}{3}(2\pi)^{1/2}(Y_4^2-Y_4^{-2}),$$
$$b_{245}=\tfrac{1}{6}(2\pi)^{1/2}(Y_4^1-7^{1/2}Y_4^{-3});$$

$n=6$:

$$b_{263}=\frac{2\sqrt{\pi}}{(13)^{1/2}}\left\{\frac{(10)^{1/2}}{16}Y_6^{-1}-\frac{9}{16}Y_6^3+\frac{(165)^{1/2}}{16}Y_6^{-5}\right\},$$

$$b_{264}=\frac{2\sqrt{\pi}}{(13)^{1/2}}\frac{(Y_6^2-Y_6^{-2})}{\sqrt{2}},$$

$$b_{265}=\frac{2\sqrt{\pi}}{(13)^{1/2}}\left\{-\frac{(10)^{1/2}}{16}Y_6^1+\frac{9}{16}Y_6^{-3}-\frac{(165)^{1/2}}{16}Y_6^5\right\}.$$

For $n=6$ a second set of spherical harmonics transforming as Γ_{5g} exists, and has to be taken into account:

For Γ_{5g}', $n=6$:

$$b_{363}=\frac{2\sqrt{\pi}}{(13)^{1/2}}\left\{\frac{3(22)^{1/2}}{16}Y_6^{-1}+\frac{(55)^{1/2}}{16}Y_6^3+\frac{\sqrt{3}}{16}Y_6^{-5}\right\},$$

$$b_{364}=\frac{2\sqrt{\pi}}{(13)^{1/2}}\frac{(Y_6^6-Y_6^{-6})}{\sqrt{2}},$$

$$b_{365}=\frac{2\sqrt{\pi}}{(13)^{1/2}}\left\{-\frac{3(22)^{1/2}}{16}Y_6^1-\frac{(55)^{1/2}}{16}Y_6^{-3}-\frac{\sqrt{3}}{16}Y_6^5\right\}.$$

Each of these seven sets of basis functions can be grouped together and therefore needs only one potential coefficient.

Defining the coefficients:

$a_{1i}\equiv$ coefficients of Γ_{3g}, $i=2, 4, 6$;
$a_{2i}\equiv$ coefficients of Γ_{5g}, $i=2, 4, 6$;
$a_{36}\equiv$ coefficient of Γ_{5g}',

we finally obtain Eq. (7).

Although Eq. (7) appears to be a complicated expression with seven phenomenological constants a_{12}, a_{14}, $\cdots$, etc., it reduces to a relatively simple form for a wave propagating along a symmetry axis. Thus, for a longitudinal wave along crystallographic [100] direction, only three unknown coefficients will be involved, and only two are needed to describe the interaction of ϵ_{xy} transverse wave with $J=\frac{5}{2}$ Ce^{3+} and Sm^{3+} ions. In this case the interaction Hamiltonian becomes

$$\mathcal{H}_{s-p}=(6\pi)^{1/2}\epsilon_{xy}\left[a_{22}\frac{\alpha}{\sqrt{5}}\bar{O}^{-2}+a_{24}\frac{\beta}{3}\bar{O}^{-4}\right]. \qquad \text{(A5)}$$

Here α, β are operator equivalent factors introduced by Stevens[35] and $\bar{O}_2^{-2}$, $\bar{O}_4^{-4}$ are angular-momentum operators whose matrix elements are proportional to $-i(Y_2^2-Y_2^{-2})$ and $-i(Y_4^4-Y_4^{-4})$. They are related to the usual operators O_n^m by

$$\langle J_z'|\bar{O}_n^{-m}|J_z\rangle=i\langle J_z'|O_n^m|J_z\rangle; \qquad \text{(A6)}$$

a complete set of matrix elements of these operators has been evaluated by Mikkelson and Stapleton.[36] Quantum numbers J_z, J_z', within the same J manifold, characterize the energy levels $|J,J_z\rangle$ and $|J,J_z'\rangle$ between which the orbit-lattice interaction, Eq. (7), induces transitions. If the static crystalline parameters $A_4\langle r^4\rangle$ and $A_6\langle r^6\rangle$ are accurately known, the ordering of levels and the wave functions can be found from the work by Lea, Leask, and Wolf.[18] The matrix elements of Eq. (7) can then be evaluated, and a_{ij} coefficients,

---

[34] J. S. Griffith, *The Theory of Transition Metal Ions* (Cambridge University Press, New York, 1961).

[35] K. W. H. Stevens, Proc. Phys. Soc. (London) **A65**, 209 (1952).

[36] R. C. Mikkelson and H. J. Stapleton, Department of Physics, University of Illinois (unpublished). (Tables are available from the authors upon request.)

are obtained from experiments. The static crystalline parameters are usually determined from the optical spectra, but in CaF_2 the optical spectra are complicated by the presence of satellite lines, and by the existence of local fields of different symmetries due to charge compensation. If the ground state is Γ_8, and if Γ_8 occurs more than once in the decomposition of the ground J manifold, the wave functions may be determined from the spin-resonance experiments. Some of the wave functions and a survey of crystalline-field parameters for rare-earth ions in CaF_2 are given in the first article of Ref. 24.

PHYSICAL REVIEW VOLUME 146, NUMBER 1 3 JUNE 1966

Effective Mass of Positrons in Metals

D. R. HAMANN
Bell Telephone Laboratories, Murray Hill, New Jersey

(Received 22 December 1965)

The self-energy of a positron in an electron gas due to electron-positron correlations is calculated to the lowest order in the dynamically screened interaction. It is shown that the dressed positron quasiparticle can be described by an effective mass, but that the calculated effective mass is much too small to account for that measured by observing thermal effects in positron-annihilation experiments. Corrections due to more complicated self-energy processes and to electron-exchange interactions are estimated and found to be small.

1. INTRODUCTION

POSITRON annihilation has been studied as a means of gaining information about the band structure of metals. In addition, however, such experiments provide an example of a distinguishable test charge interacting with a many-electron system, and we shall deal here with a particular feature of the correlations in this combined system.

The possibility of studying low-energy aspects of positron annihilation arises from the fact that the positron lifetime is long compared to the time it takes a positron injected into a metal to reach equilibrium with the electrons.[1] Suppose we naively neglect all interactions and consider an electron gas at 0°K containing a positron in its zero-momentum state. The two gamma rays produced when the positron annihilates with one of the electrons will carry away just the momentum of that electron. Angular-correlation measurements of the z component of the momentum of each gamma-ray pair should then give a distribution equal to that of the z components of the electron momenta—an inverted parabola with a cutoff at $k_z=k_F(\hbar=1)$. Now suppose this system is heated. The positron will have a Maxwellian velocity distribution, and its average momentum will be $(T/T_F)^{1/2}k_F$. The average increase in momentum for electrons at the Fermi surface will be $(T/T_F)k_F$, so for a typical T of 10^2°K and T_F of 10^5°K, the thermal smearing of the momentum-distribution cutoff will be due almost entirely to the momentum of the positron.

In actual metals, observed positron lifetimes are an order of magnitude shorter than those predicted by the noninteracting model.[1] This suggests that the interaction profoundly disturbs the momentum distribution of electrons in the vicinity of the positron. It is a paradox of this problem that the momentum fluctuations of the electrons and positron cancel in just such a way that the observed momentum distributions (from simple s-p conduction bands) reproduce almost exactly the parabola of the naive model. Kahana and co-workers have calculated the interaction effects on both the lifetime and the momentum distribution, and have obtained reasonable agreement with experimental observations in several approximations.[2] In considering the thermal smearing of the momentum distribution cutoff, we can completely avoid the complexities of these calculations by the following argument: Since the correlation effects do, in fact, cancel in the momentum distribution, only the average momentum of the positron as it undergoes various virtual transitions enters into the thermal smearing. The quasiparticle formed by the positron and its screening cloud of electrons will have a Boltzmann distribution in energy. Therefore, calculating the quasiparticle E-versus-k relationship (which hopefully may be expressed by an effective mass) should permit a complete description of the thermal smearing. This physical argument is supplemented by the recent work of Majumdar, which establishes with great generality the existence of a sharp break in the gamma-ray momentum distribution at 0°K, and the possibility of measuring the positron effective mass through the thermal smearing of this break.[3] One experiment of this sort has been carried

---

[1] R. A. Ferrell, Rev. Mod. Phys. **28**, 308 (1956).

[2] S. Kahana, Phys. Rev. **117**, 123 (1960); **129**, 1622 (1963); J. P. Carbotte and S. Kahana, *ibid.* **139**, A213 (1965).

[3] C. K. Majumdar, Phys. Rev. **140**, A227 (1965); **140**, A237 (1965).

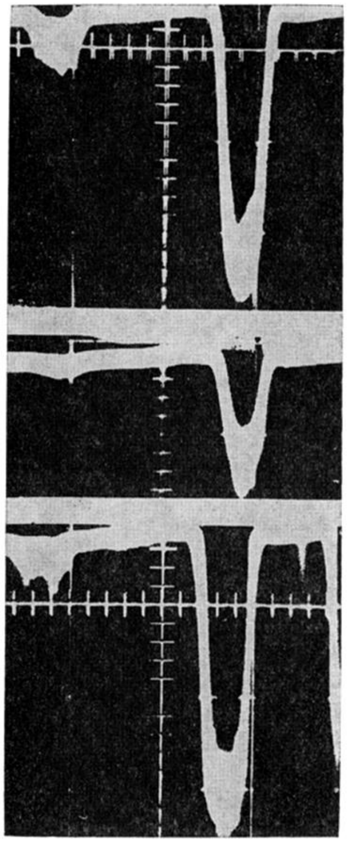

FIG. 2. Demonstration of paramagnetic resonant absorption of 10-kMc/sec transverse acoustic waves generated by ferromagnetic resonance in a thin film. Cobalt film was deposited on 0.17% concentrated ruby substrate. Upper picture: above ruby resonance $H=5280$ Oe; middle picture: on resonance $H=5200$ Oe; lower picture: below resonance $H=5120$ Oe.